

Article

Suppression of *Transferrin* Expression Enhances the Susceptibility of *Plutella xylostella* to *Isaria cicadae*

Huihui Xu ^{1,†}, Zhongping Hao ^{2,†} , Lifang Wang ³, Shuangjiao Li ¹, Yuruo Guo ¹ and Xiangli Dang ^{1,*}

¹ Key Laboratory of Biology and Green Control of Plant Diseases and Insect Pests of Anhui Higher Education Institutes, School of Plant Protection, Anhui Agricultural University, Hefei 230036, China; xh15755396709@163.com (H.X.); lsj0926@sohu.com (S.L.); guoyurrrrrruo@outlook.com (Y.G.)

² Crop Research Institute, Anhui Academy of Agricultural Sciences, Hefei 230031, China; hzp5187@sina.com

³ School of Horticulture, Anhui Agricultural University, Hefei 230036, China; wlf2000@ahau.edu.cn

* Correspondence: xldang@ahau.edu.cn

† These authors contributed equally to this work.

Received: 3 March 2020; Accepted: 2 May 2020; Published: 5 May 2020



Abstract: Transferrins (Trfs) are multifunctional proteins with key functions in iron transport. In the present study, a *Trf* (*PxTrf*) from *Plutella xylostella* was identified and characterized. The *PxTrf* consisted of a 2046-bp open reading frame, which encoded a 681 amino acid protein with a molecular weight of 73.43 kDa and had an isoelectric point of 7.18. Only a single iron domain was predicted in the N-lobe of *PxTrf*. Although *PxTrf* was expressed ubiquitously, the highest levels of expression were observed in the fourth instar larvae. *PxTrf* transcript level was highest in fat bodies among various tissues. The *PxTrf* transcript levels increased significantly after the stimulation of pathogens. A decrease in *PxTrf* expression via RNA interference enhanced the susceptibility of *P. xylostella* to the *Isaria cicadae* fungus and inhibited hemocyte nodulation in response to the fungal challenge. In addition, a considerable increase in the pupation rate was observed in larvae treated with double-stranded *PxTrf* (ds*PxTrf*). Overall, according to the results, *PxTrf* may participate in *P. xylostella* immunity against fungal infection and insect development.

Keywords: *Plutella xylostella*; *Isaria cicadae*; transferrin; expression patterns; immunity; development; RNAi

1. Introduction

The diamondback moth, *Plutella xylostella* (L.) (Lepidoptera: Plutellidae), is a notorious pest in cruciferous crops and causes an annual economic loss of \$4–5 billion [1]. Due to widespread use of insecticides, *P. xylostella* has evolved resistance against various classes of insecticides and some biopesticides, and has become one of the most insecticide-resistant pests globally [2,3]. Therefore, novel *P. xylostella* management strategies are required urgently, and biological control technologies present the greatest potential for the sustainable and efficient control of *P. xylostella* [4,5].

Entomopathogenic fungi are vital group of microorganisms that have been exploited as biological control agents against insect pests [6]. The use of entomopathogenic fungi or virulence factors produced by pathogens as pest control is one of the frontiers of biological pest control [7]. However, the effective utilization of the pathogens lies in understanding mechanisms underlying the immune defense responses of host insects to fungi. A pathogenic fungus, *Isaria cicadae*, parasitizes lepidopteran insects, such as *P. xylostella* [8]. To better understand the mechanism of *P. xylostella* immunity, we investigated the immunotranscriptome of *P. xylostella* against *I. cicadae* and identified numerous immunity-related

genes. Among immune effector genes, a transferrin (*Trf*) homolog (designated as *PxTrf*) was identified in the *P. xylostella* immunotranscriptome, which exhibited high similarity to insect *Trfs*.

Iron is a key trace element nutrient that participates in various biological processes, such as oxygen and electron transport, ATP generation, cell proliferation, detoxification, gene regulation, and DNA biosynthesis [9–11]. In insects, it is also involved in cuticle formation, tanning, melanization, wound healing, and immunity [9]. Due to the adverse effects of excessive or inadequate iron, organisms develop strategies to balance iron concentrations. Numerous proteins, such as transferrins (*Trfs*), ferritins, iron regulatory proteins, hepcidins, and matriptases, are involved in the transport and metabolism of iron [12]. As a glycoprotein family, *Trf* family members are the major iron-containing proteins that perform key iron binding and transportation functions [9]. *Trfs* are widespread in invertebrates and vertebrates. Mammalian *Trf* and lactoferrin are the two most understood *Trf* family members [13]. In addition to its iron transport and metabolism functions, mammalian *Trf* is a growth factor and a transcriptional regulator of gene expression [9]. In addition, lactoferrin plays key roles in the immune system, for example, bactericidal activity and the nuclear factor- κ B (NF- κ B) activation [14]. Further studies have showed that the *Trf* family has broad functions and participates in cellular respiration and energy balance [15].

Insect *Trf* sequences are similar to mammalian *Trf* and lactoferrin sequences. However, they only retain one iron-binding site in the N-terminal domain [9]. In addition to iron metabolism, insect *Trfs* have functions in development and stress defense [16–18]. Numerous studies have revealed that insect *Trfs* can also have a role in immunity [9]. *Trf* are upregulated transcriptionally by microbial challenge in numerous insects [19–23]. *Bombyx mori* recombinant *Trf* protein exhibits an iron binding capacity and antibacterial activity [22]. Iron-free *Manduca sexta* *Trf* inhibits bacterial growth, whereas iron-saturated *Trf* exhibits no detectable antibacterial activity [23]. Lehane et al. (2008) reported that the knockdown of *Glossina morsitans Trf* by RNA interference (RNAi) would increase trypanosome infections significantly [24]. Although insect *Trf* has been suggested to have some immune functions, its immunological function during fungal infection has not been explored.

In the present study, we report the characterization and functional analysis of *PxTrf*. *PxTrf* was cloned and its sequence was analyzed using bioinformatics tools. The expression profiles of *PxTrf* in various tissues, at various developmental stages, and under different pathogen challenges, were examined through reverse transcriptase quantitative PCR (RT-qPCR). The immunological functions of *PxTrf* were further explored by RNAi with double-stranded *PxTrf* (ds*PxTrf*) injection and subsequent immunological assays in response to *I. cicadae* infection. The efficacy of *PxTrf* on haemocyte nodule formation and larval pupation was also evaluated by injecting ds*PxTrf*. The results of the present study can enhance our understanding of the roles of *PxTrf* in the immune responses of *P. xylostella* against *I. cicadae* and its potential as a novel target of insect-specific control agents.

2. Materials and Methods

2.1. Insects and Microorganisms

Diamondback moths, *Plutella xylostella* (L.), were reared on bok choy (*Brassica rapa chinensis*) seedlings at 25 ± 1 °C, $75\% \pm 5\%$ relative humidity, and a 16:8 h (light/dark) photoperiod. Adults were provided with 10% (w/v) honey solution and allowed to lay eggs on bok choy seedlings.

The Gram-positive bacterium *Staphylococcus aureus* and the Gram-negative bacterium *Escherichia coli* were cultured in Luria–Bertani broth at 37 °C. The entomopathogenic fungus, *Isaria cicadae*, was cultured in potato dextrose agar medium at 28 °C.

2.2. cDNA Cloning

Total RNA was extracted from the fourth instar larvae of *P. xylostella* using Trizol reagent (Takara, Beijing, China) according to the manufacturer's protocol. The quality and concentrations of RNA were evaluated using a NanoDrop 2000 spectrophotometer (Thermo Scientific, Waltham, MA, USA).

First-strand complementary DNA (cDNA) was synthesized with 2 µg of total RNA by using the PrimeScript 1st Strand cDNA Synthesis Kit (Takara, Beijing, China). The coding sequence of *PxTrf* was cloned from cDNA by using specific designed primers (Table 1). PCR products were purified using an gel purification of DNA kit (Omega, Bio-tek, Norcross, GA, USA) and sequenced by General Biosystems Corporation Limited, Chuzhou, China).

Table 1. Nucleotide sequences of primers used in this study.

| Primers | Sequence (5'–3') | Function |
|------------------|---|----------|
| <i>PxTrf</i> -CF | ATCAGTGACCATGATAGTGAAAATAGCCAT | Cloning |
| <i>PxTrf</i> -CR | GTATGTATGTTTATGCAACACCACAAGATG | |
| <i>PxTrf</i> -QF | TAGCGTCAGCATCCAACAAG | qRT-PCR |
| <i>PxTrf</i> -QR | TCCAAGCTTTTTCAGGCACT | |
| <i>Actin</i> -F | TGGCACCAACACCTTCTAC | qRT-PCR |
| <i>Actin</i> -R | CATGATCTGGGTCATCTTCT | |
| <i>dsTrf</i> -F | TAATACGACTCACTATAGGGTGTGCGGAAGTTCTTTGGG | RNAi |
| <i>dsTrf</i> -R | TAATACGACTCACTATAGGGCTACGTTATCACCTGTAGGGTT | |
| <i>dsGFP</i> -F | TAATACGACTCACTATAGGGAGGGCGAGGGCGATGCCACC | RNAi |
| <i>dsGFP</i> -R | TAATACGACTCACTATAGGGTGTACTCCAGCTTGTGCCCC | |

The bold sequences represent T7 promoter sequence.

2.3. Sequence Analysis of *PxTrf*

The *PxTrf* nucleotide sequence was entered into Open Reading Frame Finder (<http://www.ncbi.nlm.nih.gov/gorf/gorf.html>) to identify open reading frames (ORFs). Signal peptides were predicted using SignalP 5.0 (<http://www.cbs.dtu.dk/services/SignalP/>), and transmembrane domains of deduced proteins were predicted using TMHMM 2.0 (<http://www.cbs.dtu.dk/services/TMHMM/>), and conserved domains were predicted using SMART (<http://smart.embl-heidelberg.de/>). Theoretical isoelectric point (pI) and molecular weight were calculated using PeptideMass (https://web.expasy.org/peptide_mass/). The glycosylation site was predicted using DictyOGlyc (<http://www.cbs.dtu.dk/services/DictyOGlyc/>). The coiled coil regions were analyzed by COILS (https://embnet.vital-it.ch/software/COILS_form.html). Protein homology modeling was performed using Swiss Model Workspace (<https://swissmodel.expasy.org/>). *PxTrf* and its orthologs from other insect species were aligned using DNAMAN 7.0. On the basis of the alignment of whole sequences of insect Trfs, a phylogenetic tree was constructed using MEGA 7.0 using the neighbor-joining method with 1000 bootstrap replications [25].

2.4. Reverse Transcriptase Quantitative PCR

RT-qPCR was performed to determine the expression profiles of *PxTrf* at various developmental stages, in different tissues, and under different microbial challenges. Total RNA was extracted separately from the *P. xylostella* eggs, first to fourth instar larvae, pupae, and adults. In addition, total RNA was extracted from the malpighian tubules, epidermis, midguts, fat bodies, and hemocytes of the fourth instar larvae. Furthermore, the fourth instar larvae were treated with *S. aureus* (1.0×10^6 colony-forming unit (cfu)/larva), *E. coli* (1.0×10^6 cfu/larva), and *I. cicadae* spore suspensions (1.0×10^7 cfu/larva). Double-distilled water (ddH₂O) was used to inject control, and naïve larvae were used as blank controls. Subsequently, they were raised under the conditions mentioned above for 24 h. Each treatment had three independent replicates.

Total RNA isolation and cDNA synthesis were performed using the methods mentioned above. RT-qPCR was performed using SYBR Premix Ex Taq™ II (Takara, Beijing, China) on a Bio-Rad CFX96 (Bio-Rad, Hercules, CA, USA). The qPCR was performed using a mixture (20 µL) of 10 µL SYBR Premix Ex Taq™ II, 0.5 µL of each primer (0.5 µM), 1 µL (200 ng) of cDNA, and 8 µL of diethylpyrocarbonate (DEPC)-ddH₂O. PCR cycling conditions were as follows: denaturation at 94 °C for 5 min, followed by 40 cycles of 95 °C for 10 s, and 60 °C for 20 s. *Actin* was employed as the reference gene. Primers are listed in Table 1. Relative *PxTrf* transcript levels (fold changes) were measured using the $2^{-\Delta\Delta C_t}$ method.

2.5. Identification of PxTrf Protein in *P. xylostella*

Naïve larvae and *I. cicadae* (1.0×10^7 cfu/larvae)-challenged larvae (24 h) were homogenized with precooled phosphate buffer saline (PBS) and centrifuged at $10,000 \times g$ for 30 min at 4 °C. The supernatants were used for protein identification. PxTrf protein was identified through liquid chromatography–tandem mass spectrometry (LC–MS/MS) according to a previously described method [26]. On the basis of combined MS and MS/MS spectra, protein was successfully identified on the basis of a 95% or higher confidence interval of their scores in the MASCOT V2.3 search engine (Matrix Science Ltd., United Kingdom). The relative quantitation of PxTrf was estimated using the exponentially modified protein abundance index (emPAI) method [27]. The emPAI is defined as follows:

$$\text{emPAI} = 10^{\text{PAI}} - 1 \quad (1)$$

where PAI is equal to the number of observed peptides per protein divided by the number of observable peptides per protein.

2.6. RNA Interference

A template corresponding to nucleotides 729–1606 of *PxTrf* for in vitro transcription reactions was prepared through PCR amplification by using gene-specific primers (Table 1). Double-stranded PxTrf (dsPxTrf) was prepared using the TranscriptAid T7 High Yield Transcription Kit (Thermo Scientific, Waltham, MA, USA) according to the manufacturer's instructions. The reaction mixture included 2 µL 10 × reaction buffer, 8 µL of nucleotide triphosphate (NTP) mixture, 1 µg of the template, and 2 µL of enzyme mix, which was supplemented with nuclease-free water up to a 20 µL volume. After overnight incubation at 37°C, the reaction mixture was isolated and purified with saturated phenol/chloroform. All synthesized double-stranded RNAs (dsRNAs) were dissolved in nuclease-free water and stored at –80°C until use. The quantity and purity of dsRNA were determined using a NanoDrop 2000 spectrophotometer (Thermo Scientific, Waltham, MA, USA). The dsGFP corresponding to green fluorescence protein (GFP) was prepared as previously mentioned using the primers (Table 1).

Two microliters of dsPxTrf (5 µg/larva) was injected into the third instar larvae of *P. xylostella* using an IM-31 Microinjector (Narishige Group, Japan). Larvae injected with similar dsGFP amount were considered controls. A DEPC-treated water (2 µL/larva) injection was considered an injection control. After injection, the larvae were raised under the conditions mentioned above. The effects of *PxTrf* silencing at different time intervals (0, 6, 12, 24, 36, and 48 h) were analyzed through RT-qPCR, as described above.

2.7. Hemocyte Nodulation Assay

The influence of dsPxTrf treatment on hemocyte nodulation was analyzed using a previously described method [28]. The third instar larvae were injected with dsPxTrf, as described previously. Injection of DEPC-treated water was the injection control, and dsGFP injection was considered a control. Six hours after treatment with dsRNA, the larvae were injected with heat-killed *I. cicadae* spore suspensions (1.0×10^8 cfu/mL). After 10 h of incubation at 25 °C, the nodule numbers were assessed under an Eclipse Ti microscope (Nikon, Tokyo, Japan). Each treatment had three replicates.

2.8. Larvae Pupation Analysis

The third instar larvae (30 larvae) were injected with dsPxTrf, as described above. After injection, they were raised under the conditions mentioned above. Pupation rates of dsRNA-treated larvae were assessed at different time intervals (0, 12, 24, 36, and 48 h). Each treatment had three replicates.

2.9. *I. cicadae* Bioassay

The third instar larvae (30 larvae) were injected with dsPxTrf, as described above. After 6 h, larvae were dipped in *I. cicadae* spore suspensions (1.0×10^8 cfu/mL) for 20 s. After infection, larvae were

maintained under the conditions mentioned above. Larvae mortality was determined until larvae developed into pupae. Larvae were considered dead when they did not move in response to touch. The experiments were performed three times.

2.10. Statistical Analysis

All data are represented as the mean ± standard error. One-way analysis of variance with Duncan’s new repolarization test was performed to compare differences among multiple samples by using the data processing system [29]. The level of significance was set at $p < 0.05$. Survival plot was generated using GraphPad Prism v8.2.1, where p -values were determined by Gehan–Breslow–Wilcoxon test.

3. Results

3.1. cDNA Cloning and Sequence Analysis of PxTrf

A contig (CL847) homologous to insect transferrin was identified in the *P. xylostella* immunotranscriptome against infection by *I. cicadae*. The *PxTrf* cDNA sequence consists of 2254 bp and the open reading frame is 2046 bp (accession no. MN928614), which encodes 681 amino acids (aa) with a 19-aa signal peptide (Figure 1). No transmembrane structure was found in *PxTrf*. The molecular weight of *PxTrf* without the signal peptide is estimated to be 73.43 kDa (monoisotopic mass), and the theoretical pI is 7.18. Two conserved Trf motifs (N- and C-lobes) are predicted in each half of the protein. The secondary structure is mostly random coil, 28.93% is the α helix, and 19.24% is the extended strand (Figure S1). *PxTrf* amino acids are similar to human Trf and lactoferrin (Figure S2). These proteins have two lobes, and the N- and C-lobe of *PxTrf* are S₂₂–V₃₅₉ and V₃₇₁–A₆₇₀, respectively. Only a single iron domain is located in the N-lobe of *PxTrf*, which includes four conserved active sites (Figure 1). Ten and four conserved cysteines were observed in the N- and C-lobes of *PxTrf*, and human Trf and lactoferrin, respectively (Figure S2). In addition, four putative glycosylation sites were observed in the Trf sequence, with each lobe having two sites (Figure 1).

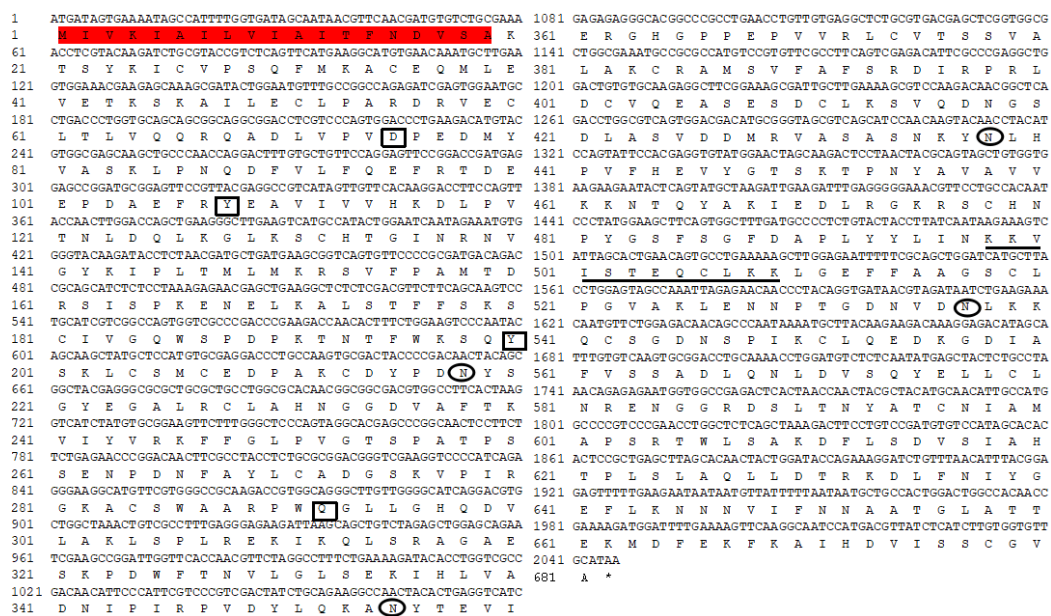


Figure 1. Nucleotide and deduced amino acid sequences of *Plutella xylostella* transferrin (*PxTrf*). Signal peptide is highlighted in red. Iron binding sites are denoted by black rectangles. Putative glycosylation sites are denoted by black oval. The nuclear localization signal is shown by underlining.

The results of the sequence alignment analysis revealed that most amino acids in the Trf sequence were conserved among the lepidopteran Trfs, particularly in the N-lobe (Figure S3). PxTrf exhibited the highest sequence similarity with *B. mori* Trf. A neighbor-joining phylogenetic tree was constructed to compare the relationship between PxTrf and other insect Trfs (Figure 2). On the basis of the tree, each insect order formed an independent clade, including Coleoptera, Orthoptera, Isoptera, Hemiptera, Hymenoptera, and Lepidoptera. PxTrf was clustered with Trf homologs from lepidopteran insects (such as *Bombyx mandarina*, *B. mori*, *Galleria mellonella*, *Papilio machaon*, and *Papilio xuthus*), and was closely related to Trfs in insects from other *Bombyx* species.

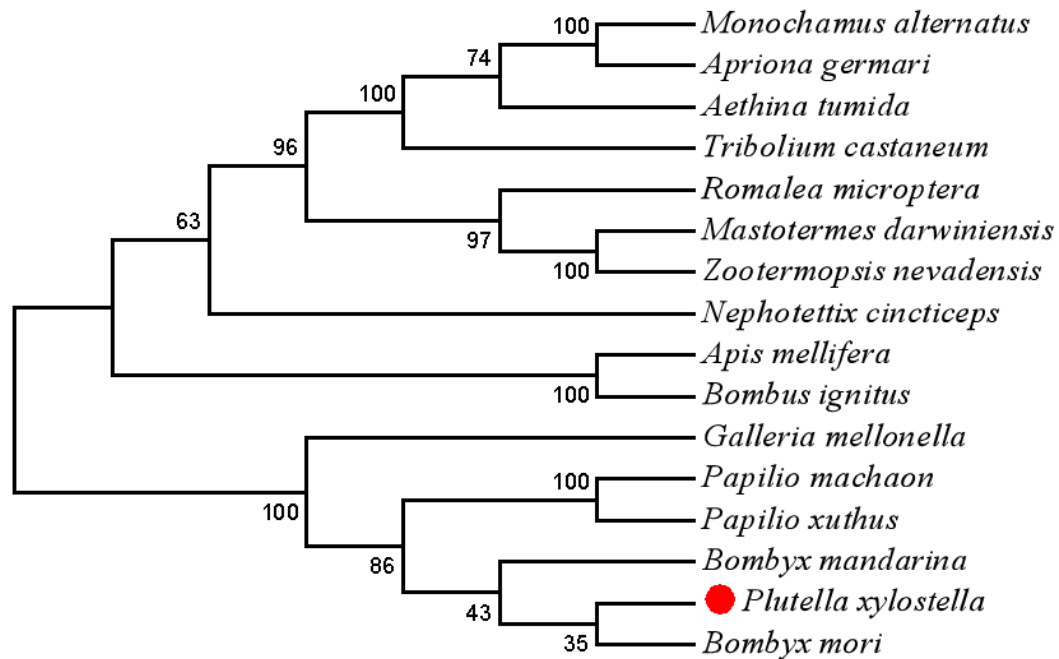


Figure 2. A neighbor-joining phylogenetic tree of *Plutella xylostella* transferrin (Trf) with other insect Trfs using MEGA 7.0. Bootstrap values from 1000 replications are displayed for each branch.

3.2. Expression Profiles of PxTrf

The *PxTrf* expression patterns at different developmental stages, in different tissues, and under different microbial challenges were determined through RT-qPCR. The highest levels of *PxTrf* transcript were observed in the fourth instar larvae, followed by the pupae, the third instar larvae, and the adults (Figure 3A). *PxTrf* was transcribed at low levels in the eggs, as well as in the first and second instar larvae. All *P. xylostella* tissues expressed *PxTrf*. High transcript levels were found in the fat bodies, epidermis, and hemocytes, with low levels in the midguts and malpighian tubules (Figure 3B). Among various tissues, the highest *PxTrf* transcript levels were observed in the fat bodies. Compared with the control and ddH₂O groups, *PxTrf* transcript levels were up-regulated significantly after induction by *S. aureus*, *E. coli*, and *I. cicadae* (Figure 3C). The *PxTrf* transcript level after induction by *I. cicadae* was approximately fivefold that of the control.

3.3. Identification of PxTrf Protein in *P. xylostella*

Extracted protein (20 µg) of naïve larvae (Naïve) and *I. cicadae*-challenged larvae (IC) of *P. xylostella* were analyzed through SDS-PAGE (Figure S4) and used for protein identification. According to LC-MS/MS results, *PxTrf* protein was identified both in Naïve and IC samples. On the basis of the emPAI values, the relative quantitation of *PxTrf* in the IC sample was 0.52, which was more than twofold that in Naïve larvae (emPAI = 0.23) (Table 2). The result is consistent with *PxTrf* expression levels based on qRT-PCR.

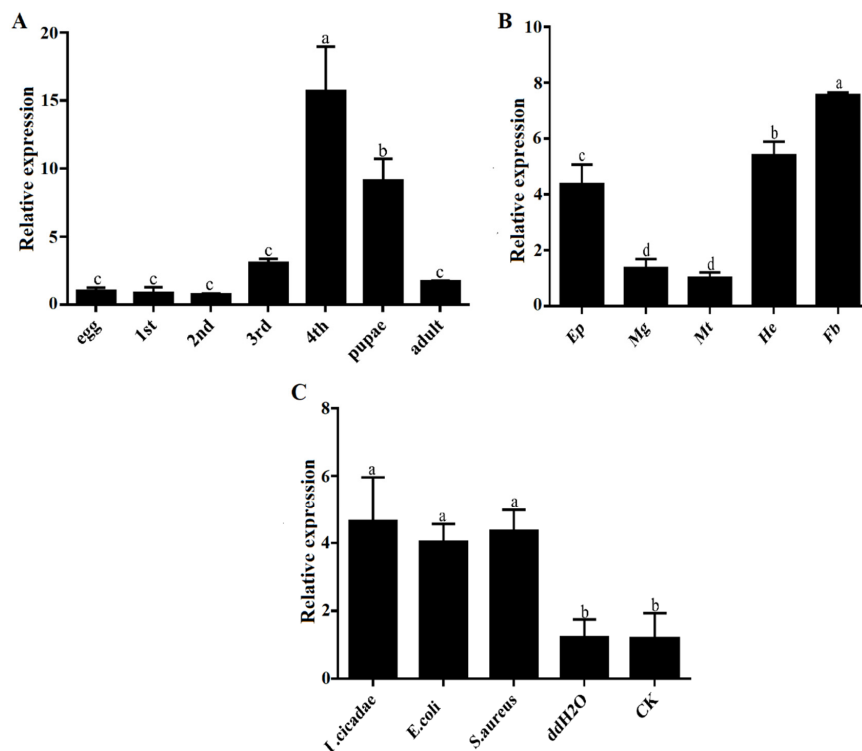


Figure 3. Relative expression levels of *PxTrf*. (A) Different developmental stages. Total RNA was extracted from the whole body of *P. xylostella*. (B) Different tissues of the fourth instar larvae. Ep: epidermis; Mg: midguts; Mt: malpighian tubules; He: hemocytes; Fb: fat bodies. (C) Different microbial challenges of the fourth instar larvae. Data are presented as the mean of three replicates ± standard error. Different lowercase letters indicate significant variations in transcription among different samples ($p < 0.05$).

Table 2. Identification of *PxTrf* protein in *P. xylostella*.

| Sample | Protein | Score | Matches | Sequences | emPAI |
|--------|-------------|-------|---------|-----------|-------|
| Naïve | Transferrin | 167 | 9 (6) | 8 (5) | 0.23 |
| IC | Transferrin | 290 | 22 (13) | 15 (10) | 0.52 |

Score: score of protein identification. Matches: number of matched mass spectra (number with reliability greater than 95%). Sequences: number of matched peptide sequences (number with reliability greater than 95%).

3.4. Analysis of the Efficacy of *PxTrf* RNAi

A *Trf*-specific dsRNA of *P. xylostella* was synthesized in vitro and injected into the third instar larvae. To quantify RNAi efficacy, a RT-qPCR assay was performed. The results showed that compared with the dsGFP (control) and DEPC-treated water (injection control), the *PxTrf* transcription level decreased markedly following ds*PxTrf* injection (Figure 4). Treatment ds*PxTrf* markedly suppressed *PxTrf* transcription 6 h post-injection, and the transcript level decreased by 67.8%. The interference effect of *PxTrf* expression decreased gradually with time, reaching a level similar to that in the dsGFP and the DEPC groups at 24 h. dsRNA-treated larvae 6 h post-injection were used in subsequent functional analyses.

3.5. Bioassay of *PxTrf* Silencing *P. xylostella* to *I. cicadae* Infection

To determine *PxTrf* function in vivo, *P. xylostella* larvae were infected with *I. cicadae* spore suspensions (1.0×10^8 cfu/mL) 6 h post-ds*PxTrf* injection. At 48 h post-infection, the survival rate of larvae without any dsRNA injection (CK+IC) was 68.9% (Figure 5). The survival rates of *P. xylostella* DEPC-treated water and dsGFP treated larvae were similar to those of the “CK+IC” group. However,

the survival rate of dsPxTrf-treated *P. xylostella* larvae was 48.9% after 48 h of infection, which was significantly lower than that of the control, and those of the DEPC water- and the dsGFP-treated groups. According to the results, injection of dsPxTrf could increase the rate of infection of the fungus *I. cicadae* to *P. xylostella*.

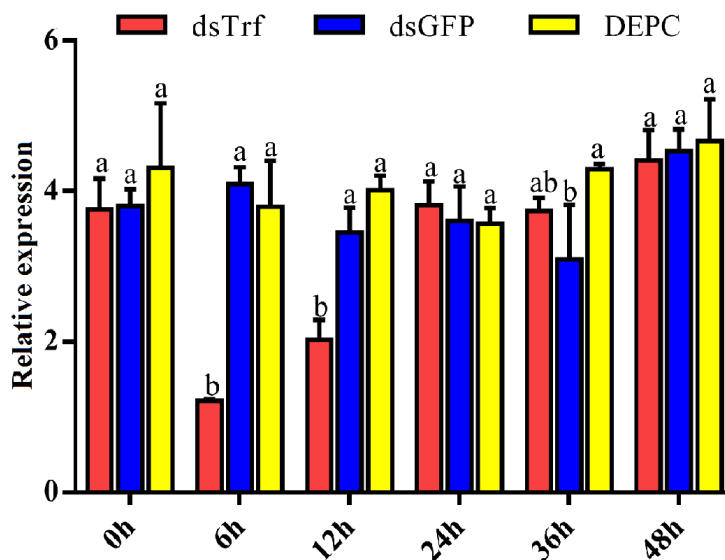


Figure 4. Analyses of the *PxTrf* expression of dsRNA-treated *P. xylostella* using RT-qPCR. dsTrf: injection double-stranded *PxTrf* (dsPxTrf). dsGFP: injection dsGFP. DEPC: injection DEPC-treated water. Data are presented as the mean \pm standard error. Different lowercase letters indicate significant variations in transcription among different samples ($p < 0.05$).

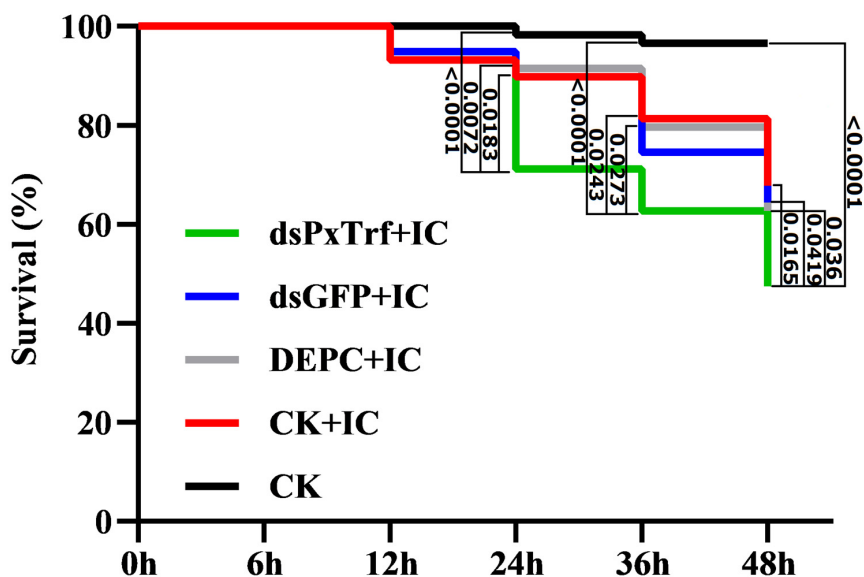


Figure 5. Survival of larvae injected dsRNA following fungal infection. CK: control (uninfection). DEPC: DEPC-treated water injection. dsGFP: dsGFP injection. dsPxTrf: dsPxTrf injection. IC: *I. cicadae* infection. p -values are presented only for the treatments with significant difference compared with the dsPxTrf injection treatment. p -values were calculated by the Gehan–Breslow–Wilcoxon test.

3.6. Hemocyte Nodulation Assay

In response to *I. cicadae* challenge, the hemocytes of *P. xylostella* without dsRNA treatment (CK) induced around 27.7 nodules per larva (Figure 6). A decrease in *PxTrf* transcription following dsRNA injection impaired nodule formation significantly ($p < 0.05$) in response to fungal challenge.

After 10 h incubation at 25 °C, only 14.3 nodules were observed in dsPxTrf-treated *P. xylostella* larvae. No significant differences were observed among CK, DEPC water, and dsGFP groups.

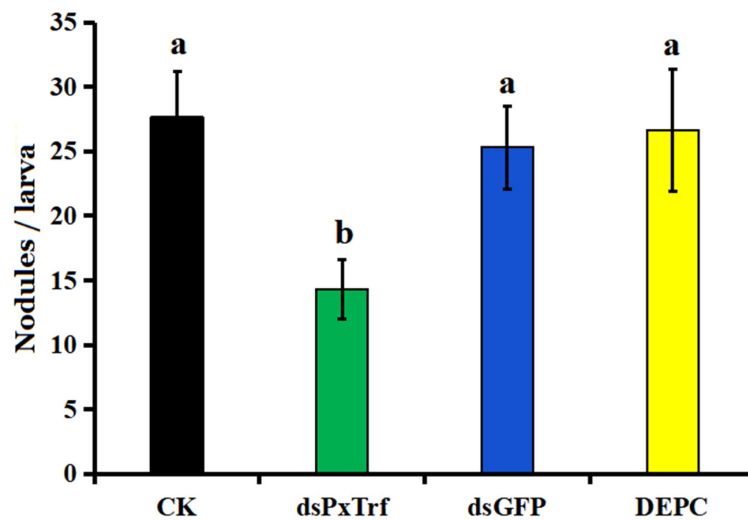


Figure 6. Influence of dsPxTrf treatment on hemocyte nodulation. CK: without dsRNA injection. dsPxTrf: dsPxTrf injection. dsGFP: dsGFP injection. DEPC: DEPC-treated water injection. Data are presented as the mean ± standard error. Different lowercase letters indicate significant variations among different samples ($p < 0.05$).

3.7. Larvae Pupation Analysis

The efficacy of *PxTrf* RNAi on larval pupation was evaluated in the third instar larvae by the injection of dsPxTrf. The results showed that the pupation rate dramatically increased in dsPxTrf-treated larvae at 12, 24, 36, and 48 h (Figure 7). At 48 h, the pupation rates of the control (CK), DEPC-treated water (DEPC), and dsGFP-treated (dsGFP) groups were 8.3%, 10.8%, and 11.7%, respectively. The pupation rates of dsPxTrf were 29.2% at 48 h, which was significantly higher than the rates in CK, DEPC, and dsGFP treatments.

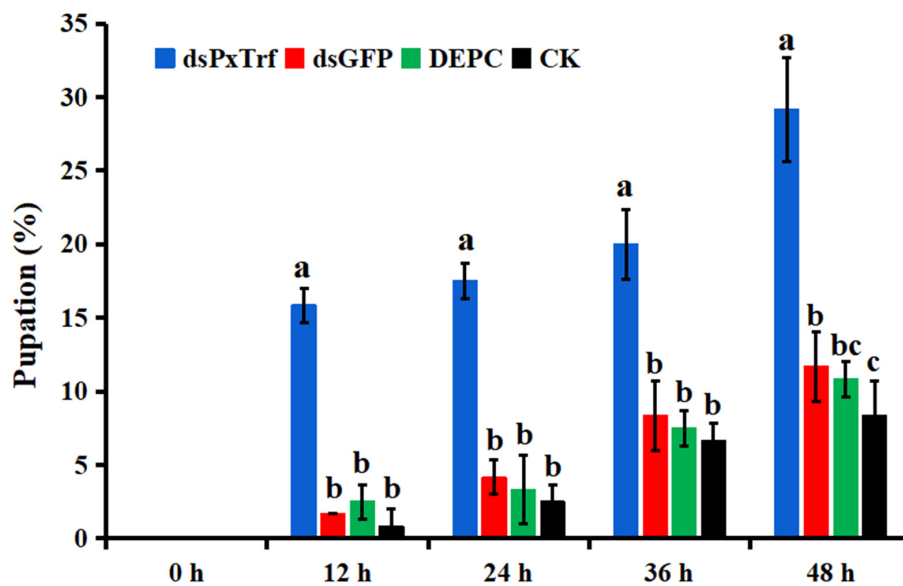


Figure 7. Pupation rate of larvae following dsPxTrf treatment. CK: without dsRNA injection. dsPxTrf: dsPxTrf injection. dsGFP: dsGFP injection. DEPC: DEPC-treated water injection. Data are presented as the mean ± standard error. Different lowercase letters indicate significant variations among different samples ($p < 0.05$).

4. Discussion

In the present study, *PxTrf* was identified from the immunotranscriptome of *P. xylostella*, which encodes 681-aa protein and exhibits high sequence similarity with other lepidopteran Trfs. Through bioinformatics analyses, we observed that *PxTrf* contains a signal peptide without a transmembrane structure. A transferrin gene (*Px-Tf*) (accession no. BAF36818) has previously been predicted from an expressed sequence tag database of *P. xylostella* [28]. Although *PxTrf* and *Px-Tf* encode the same numbers of amino acid residues, they have different molecular weights. In addition, *Px-Tf* is estimated to be 11.3 pI, whereas the pI of *Px-Trf* is only 7.18. Usually, insects have more than one *Trf* in their genomes. For instance, there are two *Trfs* in *Drosophila melanogaster*, three in *Tribolium castaneum*, and up to five in *Harpegnathos saltator* [9].

Mammalian Trfs often have 28–38 Cys residues, whereas insect Trfs have 24 or 26 Cys residues [9]. Twenty-four Cys residues were found in the *PxTrf* sequence (Figure 1). The results of alignment of *PxTrf* with mammalian lactoferrin and transferrin indicated that highly conserved Cys were mostly in the N-terminal lobe (Figure S2). The conserved Cys in their sequences form intrachain disulfide bonds, which facilitate the maintenance of Trf protein conformations. Disulfide bonds can not only stabilize the protein structure, but are also essential for the binding of iron and Trf receptor action [30].

Structurally, mammalian Trfs usually have two similar domains at the N- and C-terminals, with each containing an iron binding site. The two domains are considered to be formed by gene replication during the evolution process, which can enhance the transport of iron [31]. Although insect Trfs display structures similar to mammalian Trfs (Figure S1), most of them lose the capacity to bind iron at the C-terminal, and only retain the iron binding site at the N-terminal. The N-terminal iron binding residues D, Y, Y, and H/Q are conserved in the N-lobe of *PxTrf*, mammalian Trf, and lactoferrin (Figure S2). The C-terminal iron binding residues D, Y, Y, and H are completely conserved in the C-lobes of mammalian Trf and lactoferrin, whereas *PxTrf* lacks both Y residues (Figure S2). *M. sexta* Tsf1 is found to miss both Y and H in the C-lobe and does not exhibit iron binding activity [32]. *PxTrf* predicted only a single iron domain in the N-lobe. However, Trf of *Blaberus discoidalis* [32], *Mastotermes darwiniensis* [20], and *Protaetia brevitarsis* [33] maintain two iron binding sites in the N- and C-lobes. The function of the C-terminal is the stabilization of the Trf structure and to ensure the iron binding ability [34].

PxTrf was found to be highly transcribed in the fat bodies, hemocytes, and epidermis (Figure 3B). In addition, the highest *PxTrf* transcript levels were observed in the fat bodies, which is consistent with the findings of previous studies [18,35,36]. Insect fat bodies and hemocytes are well known to have immune properties, in which various antimicrobial peptides are synthesized in response to microbial challenges [37]. Similar to reports in other insects, *PxTrf* transcript levels increase upon bacterial and fungal challenges, suggesting that *PxTrf* participates in immunity. Notably, *PxTrf* was also found in naïve *P. xylostella* larvae, and an increase in the relative quantitation of *PxTrf* was observed in *I. cicadae*-challenged larvae. Brummett et al. (2017) also found that the concentrations of *M. sexta* Trf in the hemolymph increased from 2 to 10 μ M following an immune challenge [23]. However, most antimicrobial peptides are not found or are expressed at lower concentration in naïve insects, and are up-regulated considerably following microbial infection [38].

Insect Trf is a multifunctional protein with numerous functions, including iron transport, stress adaptation, immunity, and development [9,39]. As an iron transporter, the iron-binding activity of Trf has been studied extensively in many insects [22,32,40–42]. Putative NF- κ B binding sites are found in the promoter regions of many *Trfs*, suggesting a potential immunological function [22,35,43]. Iron is essential for the host and the pathogen, because both require the element as a cofactor or as a prosthetic group for essential enzymes [44]. The iron-sequestering strategy of host immunity is an effective antimicrobial defense mechanism that combats microbial infection by depriving microorganisms of iron [45,46]. Numerous studies have demonstrated that insect Trfs can restrict the growth of microbial pathogens in vitro [22,23]. Trf also influences bacterial biofilm formation. The addition of 50 μ g/mL of human Trf resulted in an 80% decrease in biofilm levels in *Bacillus thuringiensis* [47]. In addition,

recombinant human Trf disrupted the membrane potentials of *Acinetobacter baumannii*, *S. aureus*, and *Candida albicans* in a dose-dependent manner [48]. In vivo, insect Trf exhibited an immunological function during infection. *G. morsitans* Trf is upregulated in self-cured flies compared with flies infected with trypanosomes. Furthermore, knockdown of it results in a significant increase in trypanosome infections in the fly midgut [24]. Kim and Kim (2010) found an enhanced susceptibility to infection with a Gram-positive bacterium, *B. thuringiensis*, when *P. xylostella* Tsf1 was silenced [28]. In this study, injection of dsPxTrf could effectively silence Trf expression and enhance *P. xylostella* larvae susceptibility to the fungus *I. cicadae*. Furthermore, we observed that a decrease in PxTrf expression inhibited hemocyte nodulation significantly in response to *I. cicadae* challenge. Suppression of the *I. cicadae* Tsf1 expression also reduced nodule formation in response to bacterial challenge [28]. Therefore, PxTrf is potentially involved in *P. xylostella* immunity against fungal infection.

Trf is likely involved in insect development [9]. Studies in mammals have shown that Trf participates in development [49,50]. Nuclear localization signals are stretches of residues in proteins mediating their importing into the nucleus [51]. A nuclear localization signal was also identified in the PxTrf C-terminal domain (Figure 1), which facilitates Trf regulation of cell growth by interacting with nuclear DNA [28]. We observed PxTrf expression at various developmental stages, from eggs to adults. Higher expression levels were observed at the fourth larvae and pupae, and the lower levels occurred at the eggs, and the first and second instar larvae stages (Figure 3A). The pupation rate increased dramatically in larvae treated with dsPxTrf when compared with the control, DEPC water-, and dsGFP-treated larvae. We speculate that this insect adopts the strategy of pupation to adapt to the adverse environmental condition caused by PxTrf RNAi. Insect transferrin is regulated by juvenile hormone (JH) in many insects [9]. Generally, JH level is low in insects' pupae stage [52]. The low level of JH is also found in diapause insects, a physiological state that is used as a means to survive [9]. Zhang et al. (2015) also reported that, compared with the dsGFP control, there was a dramatic body weight decrease in *Helicoverpa armigera* larvae after feeding with Trf dsRNA for 5 days [18]. These findings indicate that Trf may participate in insect development.

5. Conclusions

In summary, we identified and characterized transferrin from *P. xylostella* and analyzed its multiple functions using RNAi. The highest PxTrf transcript levels were observed in the fourth instar larvae and fat bodies. The PxTrf transcript levels increased significantly after stimulation with pathogens in vivo. PxTrf protein was identified in both naïve and *I. cicadae*-challenged larvae. Injection with dsPxTrf increased rates of infection of *P. xylostella* with the *I. cicadae* fungus. Furthermore, suppression the Trf transcription inhibited nodule formation in response to fungal challenge significantly. In addition, a marked increase in the pupation rate was observed in larvae treated with dsPxTrf compared with the control and the dsGFP-treated larvae. According to the results of the present work, PxTrf can be involved in *P. xylostella* immunity against fungal infection and participate in insect development.

Supplementary Materials: The following are available online at <http://www.mdpi.com/2075-4450/11/5/281/s1>, Figure S1: The model structure of PxTrf. The structure was generated by protein homology modeling using Swiss Model Workspace (<https://swissmodel.expasy.org/>). (A) Human lactoferrin (Protein Data Bank (PDB) ID: 1b0l.1). (B) PxTrf, Figure S2: Alignment of the amino acid sequences of PxTrf with mammalian lactoferrin and transferrin. P: *Plutella xylostella*. H: human (*Homo sapiens*). The N- and C-lobes are indicated by red box and green box, respectively. Active sites are highlighted in yellow. Iron binding sites are denoted by star, Figure S3: Alignment of the amino acid sequences of Lepidopteran Trfs. The N- and C-lobes are indicated by red box and green box, respectively. The conserved amino acids are highlighted in black, Figure S4: SDS-PAGE of extracted protein from *P. xylostella* larvae. IC: *I. cicadae*-challenged larvae. Naïve: larvae without microbial challenge. Mr: protein molecular marker.

Author Contributions: Conceptualization, X.D.; methodology and formal analysis, X.D., H.X., and Z.H.; resources, X.D. and L.W.; investigation, H.X., Z.H., L.W., S.L., Y.G., and X.D.; writing—review and editing, X.D., H.X., and Z.H.; funding acquisition, X.D. and Z.H. All authors have read and agreed to the published version of the manuscript.

Funding: This work was supported by the National Natural Science Foundation of China (31201569), the National Key R&D Program of China (2018YFD0200905 and 2018YFD0300902-4), the State Scholarship Fund of China Scholarship Council (201808775004), and the Scientific Research Fund of Anhui Agricultural University (yj2014-7).

Conflicts of Interest: The authors declare no conflict of interest.

References

1. Li, Z.; Feng, X.; Liu, S.S.; You, M.; Furlong, M.J. Biology, ecology, and management of the diamondback moth in China. *Annu. Rev. Entomol.* **2016**, *61*, 277–296. [[CrossRef](#)] [[PubMed](#)]
2. Peres, L.L.S.; Sobreiro, A.I.; Couto, I.F.S.; Silva, R.M.; Pereira, F.F.; Heredia-Vieira, S.C.; Cardoso, C.A.L.; Mauad, M.; Scalon, S.P.Q.; Verza, S.S.; Mussury, R.M. Chemical compounds and bioactivity of aqueous extracts of *Alibertia* spp. in the control of *Plutella xylostella* L. (Lepidoptera: Plutellidae). *Insects* **2017**, *8*, 125. [[CrossRef](#)] [[PubMed](#)]
3. Zhu, B.; Li, X.; Liu, Y.; Gao, X.; Liang, P. Global identification of microRNAs associated with chlorantraniliprole resistance in diamondback moth *Plutella xylostella* (L.). *Sci Rep.* **2017**, *7*, e40713. [[CrossRef](#)] [[PubMed](#)]
4. Zhu, B.; Xu, M.; Shi, H.; Gao, X.; Liang, P. Genome-wide identification of lncRNAs associated with chlorantraniliprole resistance in diamondback moth *Plutella xylostella* (L.). *BMC Genom.* **2017**, *18*, e380. [[CrossRef](#)]
5. Li, X.; Shi, H.; Gao, X.; Liang, P. Characterization of UDP-glucuronosyltransferase genes and their possible roles in multi-insecticide resistance in *Plutella xylostella* (L.). *Pest Manag. Sci.* **2018**, *74*, 695–704. [[CrossRef](#)]
6. Hajek, A.E.; Delalibera, I. Fungal pathogens as classical biological control agents against arthropods. *Biocontrol* **2010**, *55*, 147–158. [[CrossRef](#)]
7. Levitin, A.; Whiteway, M. *Drosophila* innate immunity and response to fungal infections. *Cell. Microbiol.* **2008**, *10*, 1021–1026. [[CrossRef](#)]
8. Fang, M.; Chai, Y.; Chen, G.; Wang, H.; Huang, B. N6-(2-hydroxyethyl)-adenosine exhibits insecticidal activity against *Plutella xylostella* via adenosine receptors. *PLoS ONE* **2016**, *11*, e0162859. [[CrossRef](#)]
9. Geiser, D.L.; Winzerling, J.J. Insect transferrins: Multifunctional proteins. *Biochim. et Biophys. Acta* **2012**, *1820*, 437–451. [[CrossRef](#)]
10. Luck, A.N.; Mason, A.B. Transferrin-mediated cellular iron delivery. *Curr. Top. Membr.* **2012**, *69*, 3–35.
11. Guo, S.; Frazer, D.M.; Anderson, G.J. Iron homeostasis: Transport, metabolism, and regulation. *Curr. Opin. Clin. Nutr. Metab. Care.* **2016**, *19*, 276–281. [[CrossRef](#)] [[PubMed](#)]
12. Gkouvatso, K.; Papanikolaou, G.; Pantopoulos, K. Regulation of iron transport and the role of transferrin. *Biochim. Biophys. Acta* **2012**, *1820*, 188–202. [[CrossRef](#)] [[PubMed](#)]
13. Lambert, L.A. Molecular evolution of the transferrin family and associated receptors. *Biochim. Biophys. Acta* **2012**, *1820*, 244–255. [[CrossRef](#)] [[PubMed](#)]
14. Hughes, A.L.; Friedman, R. Evolutionary diversification of the vertebrate transferrin multi-gene family. *Immunogenetics* **2014**, *66*, 651–661. [[CrossRef](#)]
15. Ong, S.T.; Ho, J.Z.; Ho, B.; Ding, J.L. Iron-withholding strategy in innate immunity. *Immunobiology* **2006**, *211*, 295–314. [[CrossRef](#)]
16. Hirai, M.; Watanabe, D.; Chinzei, Y. A juvenile hormone-repressible transferrinlike protein from the bean bug, *Riptortus clavatus*: cDNA sequence analysis and protein identification during diapause and vitellogenesis. *Arch. Insect Biochem. Physiol.* **2000**, *44*, 17–26. [[CrossRef](#)]
17. Kim, B.Y.; Lee, K.S.; Choo, Y.M.; Kim, I.; Je, Y.H.; Woo, S.D.; Lee, S.M.; Park, H.C.; Sohn, H.D.; Jin, B.R. Insect transferrin functions as an antioxidant protein in a beetle larva. *Comp. Biochem. Physiol. B* **2008**, *150*, 161–169. [[CrossRef](#)]
18. Zhang, L.; Shang, Q.; Lu, Y.; Zhao, Q.; Gao, X. A transferrin gene associated with development and 2-tridecanone tolerance in *Helicoverpa armigera*. *Insect Mol. Biol.* **2015**, *24*, 155–166. [[CrossRef](#)]
19. De Gregorio, E.; Spellman, P.T.; Rubin, G.M.; Lemaitre, B. Genome-wide analysis of the *Drosophila* immune response by using oligonucleotide microarrays. *Proc. Natl. Acad. Sci. USA* **2001**, *98*, 12590–12595. [[CrossRef](#)]
20. Thompson, G.J.; Crozier, Y.C.; Crozier, R.H. Isolation and characterization of a termite transferrin gene up-regulated on infection. *Insect Mol. Biol.* **2003**, *12*, 1–7. [[CrossRef](#)]
21. Guz, N.; Attardo, G.M.; Wu, Y.; Aksoy, S. Molecular aspects of transferrin expression in the tsetse fly (*Glossina morsitans morsitans*). *J. Insect Physiol.* **2007**, *53*, 715–723. [[CrossRef](#)] [[PubMed](#)]

22. Yun, E.Y.; Lee, J.K.; Kwon, O.Y.; Hwang, J.S.; Kim, I.; Kang, S.W.; Lee, W.J.; Ding, J.L.; You, K.H.; Goo, T.W. *Bombyx mori* transferrin: Genomic structure, expression and antimicrobial activity of recombinant protein. *Developmental Comp. Immunol.* **2009**, *33*, 1064–1069. [[CrossRef](#)] [[PubMed](#)]
23. Brummett, L.M.; Kanost, M.R.; Gorman, M.J. The immune properties of *Manduca sexta* transferrin. *Insect Biochem. Mol. Biol.* **2017**, *81*, 1–9.
24. Lehane, M.J.; Gibson, W.; Lehane, S.M. Differential expression of fat body genes in *Glossina morsitans morsitans* following infection with *Trypanosoma brucei brucei*. *Int. J. Parasitol.* **2008**, *38*, 93–101. [[CrossRef](#)] [[PubMed](#)]
25. Kumar, S.; Stecher, G.; Tamura, K. MEGA7: Molecular Evolutionary Genetics Analysis version 7.0 for bigger datasets. *Mol. Biol. Evol.* **2016**, *33*, 1870–1874. [[CrossRef](#)]
26. Dang, X.; Zheng, X.; Wang, Y.; Wang, L.; Ye, L.; Jiang, J. Antimicrobial peptides from the edible insect *Musca domestica* and their preservation effect on chilled pork. *J. Food Process. Preserv.* **2019**, e14369. [[CrossRef](#)]
27. Ishihama, Y.; Oda, Y.; Tabata, T.; Sato, T.; Nagasu, T.; Rappsilber, J.; Mann, M. Exponentially modified protein abundance index (emPAI) for estimation of absolute protein amount in proteomics by the number of sequenced peptides per protein. *Mol. Cell. Proteom.* **2005**, *4*, 1265–1272. [[CrossRef](#)]
28. Kim, J.; Kim, Y. A viral histone H4 suppresses expression of a transferrin that plays a role in the immune response of the diamondback moth, *Plutella xylostella*. *Insect Mol. Biol.* **2010**, *19*, 567–574. [[CrossRef](#)]
29. Tang, Q.Y.; Zhang, C.X. Data Processing System (DPS) software with experimental design, statistical analysis and data mining developed for use in entomological research. *Insect Sci.* **2013**, *20*, 254–260. [[CrossRef](#)]
30. Cheng, Y.; Zak, O.; Aisen, P.S.; Harrison, C.; Walz, T. Structure of the human transferrin receptor-transferrin complex. *Cell* **2004**, *116*, 565–576. [[CrossRef](#)]
31. Lambert, L.A.; Perri, H.; Halbrooks, P.J.; Mason, A.B. Evolution of the transferrin family: Conservation of residues associated with iron and anion binding. *Comp. Biochem. Physiol. B* **2005**, *142*, 129–141. [[CrossRef](#)]
32. Jamroz, R.C.; Gasdaska, J.R.; Bradfield, J.Y.; Law, J.H. Transferrin in a cockroach: Molecular cloning characterization, and suppression by juvenile hormone. *Proc. Natl. Acad. Sci. USA* **1993**, *90*, 1320–1324. [[CrossRef](#)] [[PubMed](#)]
33. Kim, B.Y.; Lee, K.S.; Choo, Y.M.; Kim, I.; Hwang, J.S.; Sohn, H.D.; Jin, B.R. Molecular cloning and characterization of a transferrin cDNA from the white-spotted flower chafer, *Protaetia brevitarsis*. *DNA Seq.* **2008**, *19*, 146–150. [[CrossRef](#)] [[PubMed](#)]
34. Georgieva, T.; Dunkov, B.C.; Dimov, S.; Ralchev, K.; Law, J.H. *Drosophila melanogaster* ferritin: cDNA encoding a light chain homologue, temporal and tissue specific expression of both subunit types. *Insect Biochem. Mol. Biol.* **2002**, *32*, 295–302. [[CrossRef](#)]
35. Harizanova, N.; Georgieva, T.; Dunkov, B.C.; Yoshiga, T.; Law, J.H. *Aedes aegypti* transferrin. Gene structure, expression pattern, and regulation. *Insect Mol. Biol.* **2005**, *14*, 79–88. [[CrossRef](#)] [[PubMed](#)]
36. Wang, D.; Kim, B.Y.; Lee, K.S.; Yoon, H.J.; Cui, Z.; Lu, W.; Jia, J.M.; Kim, D.H.; Sohn, H.D.; Jin, B.R. Molecular characterization of iron binding proteins, transferrin and ferritin heavy chain subunit, from the bumblebee *Bombus ignitus*. *Comp. Biochem. Physiol. B* **2009**, *152*, 20–27. [[CrossRef](#)]
37. Gillespie, J.P.; Kanost, M.R.; Trenczek, T. Biological mediators of insect immunity. *Annu. Rev. Entomol.* **1997**, *42*, 611–643. [[CrossRef](#)]
38. Ezzati-Tabrizi, R.; Farrokhi, N.; Talaei-Hassanloui, R.; Alavi, S.M.; Hosseiniaveh, V. Insect inducible antimicrobial peptides and their applications. *Curr. Protein Pept. Sci.* **2013**, *14*, 698–710. [[CrossRef](#)]
39. Dunkov, B.; Georgieva, T. Insect iron binding proteins: Insights from the genomes. *Insect Biochem. Mol. Biol.* **2006**, *36*, 300–309. [[CrossRef](#)]
40. Huebers, H.A.; Huebers, E.; Finch, C.A.; Webb, B.A.; Truman, J.W.; Riddiford, L.M.; Martin, A.W.; Massover, W.H. Iron binding proteins and their roles in the tobacco hornworm, *Manduca sexta* (L.). *J. Comp. Physiol. B* **1988**, *158*, 291–300. [[CrossRef](#)]
41. Bartfeld, N.S.; Law, J.H. Isolation and molecular cloning of transferrin from the tobacco hornworm, *Manduca sexta*. *J. Biol. Chem.* **1990**, *265*, 21684–21691. [[PubMed](#)]
42. Kurama, T.; Kurata, S.; Natori, S. Molecular characterization of an insect Transferrin and its selective incorporation into eggs during oogenesis. *Eur. J. Biochem.* **1995**, *228*, 229–235. [[CrossRef](#)] [[PubMed](#)]
43. Levy, F.; Bulet, P.; Ehret-Sabatier, L. Proteomic analysis of the systemic immune response of *Drosophila*. *Mol. Cell. Proteom.* **2004**, *3*, 156–166. [[CrossRef](#)] [[PubMed](#)]
44. Schaible, U.E.; Kaufmann, S.H.E. Iron and microbial infection. *Nat. Rev. Microbiol.* **2004**, *2*, 946–953. [[CrossRef](#)]

45. Barber, M.F.; Elde, N.C. Escape from bacterial iron piracy through rapid evolution of transferrin. *Science* **2014**, *346*, 1362–1366. [[CrossRef](#)]
46. Bruhn, K.W.; Spellberg, B. Transferrin-mediated iron sequestration as a novel therapy for bacterial and fungal infections. *Curr. Opin. Microbiol.* **2015**, *27*, 57–61. [[CrossRef](#)]
47. Garner, B.; Brown, E.; Taplin, M.; Garcia, A.; Williams-Mapp, B. Transferrin impacts *Bacillus thuringiensis* biofilm levels. *Biomed. Res. Int.* **2016**, *2016*, e3628268. [[CrossRef](#)]
48. Lin, L.; Pantapalangkoor, P.; Tan, B.; Bruhn, K.W.; Ho, T.; Nielsen, T.; Skaar, E.P.; Zhang, Y.; Bai, R.; Wang, A.; Doherty, T.M.; Spellberg, B. Transferrin iron starvation therapy for lethal bacterial and fungal infections. *J. Infect. Dis.* **2014**, *210*, 254–264. [[CrossRef](#)]
49. Ned, R.M.; Swat, W.; Andrews, N.C. Transferrin receptor 1 is differentially required in lymphocyte development. *Blood* **2003**, *102*, 3711–3718. [[CrossRef](#)]
50. Macedo, M.F.; de Sousa, M.; Ned, R.M.; Mascarenhas, C.; Andrews, N.C.; Correia-Neves, M. Transferrin is required for early T-cell differentiation. *Immunology* **2004**, *112*, 543–549. [[CrossRef](#)]
51. Lin, J.R.; Hu, J. SeqNLS: Nuclear localization signal prediction based on frequent pattern mining and linear motif scoring. *PLoS ONE* **2013**, *8*, e76864. [[CrossRef](#)] [[PubMed](#)]
52. Truman, J.W.; Riddiford, L.M. The evolution of insect metamorphosis: A developmental and endocrine view. *Philos. Trans. R. Soc. B* **2019**, *374*, e20190070. [[CrossRef](#)] [[PubMed](#)]



© 2020 by the authors. Licensee MDPI, Basel, Switzerland. This article is an open access article distributed under the terms and conditions of the Creative Commons Attribution (CC BY) license (<http://creativecommons.org/licenses/by/4.0/>).